

## Observation of a gamma-ray flash at ground level in association with a cloud-to-ground lightning return stroke

J. R. Dwyer,<sup>1</sup> M. M. Schaal,<sup>1</sup> E. Cramer,<sup>1</sup> S. Arabshahi,<sup>1</sup> N. Liu,<sup>1</sup> H. K. Rassoul,<sup>1</sup> J. D. Hill,<sup>2</sup> D. M. Jordan,<sup>2</sup> and M. A. Uman<sup>2</sup>

Received 6 April 2012; revised 23 August 2012; accepted 23 August 2012; published 3 October 2012.

[1] Terrestrial gamma-ray flashes (TGFs) are bright, sub-millisecond bursts of gamma-rays, originating within the Earth's atmosphere. Most TGFs have been detected by spacecraft in low-Earth orbit. Only two TGFs have previously been observed from within our atmosphere: one at ground level and one from an aircraft at 14.1 km. We report on a new TGF-like gamma-ray flash observed at ground level, detected by the 19-station Thunderstorm Energetic Radiation Array (TERA) at the University of Florida/Florida Tech International Center for Lightning Research and Testing (ICLRT). The gamma-ray flash, which had a duration of 52.7  $\mu$ s, occurred on June 30, 2009 during a natural negative cloud-to-ground lightning return stroke, 191  $\mu$ s after the start of the stroke. This event is the first definitive association of a gamma-ray flash with natural CG lightning and is among the most direct links to a specific lightning process so far. For this event, 19 gamma-rays were recorded, with the highest energy exceeding 20 MeV. The high-energy radiation exhibited very different behavior from the typical x-ray emission from lightning. Specifically, the gamma-ray flash had a much harder energy spectrum, consistent with relativistic runaway electron avalanche (RREA) multiplication; it did not arrive in sub-microsecond bursts, typical of leader emission from lightning, and it occurred well after the start of the return stroke, which has not been previously observed for the x-ray emission from lightning. Nevertheless, we present evidence that the source region for the gamma ray flash was the same as that for the preceding leader x-ray bursts.

**Citation:** Dwyer, J. R., M. M. Schaal, E. Cramer, S. Arabshahi, N. Liu, H. K. Rassoul, J. D. Hill, D. M. Jordan, and M. A. Uman (2012), Observation of a gamma-ray flash at ground level in association with a cloud-to-ground lightning return stroke, *J. Geophys. Res.*, 117, A10303, doi:10.1029/2012JA017810.

### 1. Introduction

#### 1.1. Overview of Terrestrial Gamma-Ray Flashes (TGFs)

[2] Terrestrial gamma-ray flashes (TGFs) are intense, multi-MeV bursts of gamma-rays that originate from within the Earth's atmosphere. They were first reported by *Fishman et al.* [1994] using data from CGRO/BATSE. It was almost immediately recognized that TGFs are associated with thunderstorms, and it was later determined that TGFs are associated with individual lightning flashes [*Inan et al.*, 1996]. Because gamma-rays experience rapid attenuation in the atmosphere, it was initially hypothesized that the source of TGFs was sprites,

which are also associated with thunderstorm and lightning and have altitudes that reach about 80 km. However, it was later found by RHESSI that most TGFs originate from thundercloud altitudes, 15–21 km, and not from sprites [*Dwyer and Smith*, 2005; *Cummer et al.*, 2005; *Williams et al.*, 2006; *Carlson et al.*, 2007; *Gjesteland et al.*, 2010]. Indeed, it is now established that many TGFs are associated with positive intracloud lightning and occur when an upward leader is propagating between negative and positive charge regions within the cloud [*Stanley et al.*, 2006; *Lu et al.*, 2010; *Shao et al.*, 2010; *Cummer et al.*, 2011].

[3] Based upon BATSE data, it was initially thought that most TGFs had durations of about 1 msec. However, it is now known that instrumental saturation, coupled with Compton scattering in the atmosphere, artificially increased the measured duration of the BATSE TGFs [*Grefenstette et al.*, 2008]. Later observations by RHESSI and Fermi/GBM showed that most TGFs have durations ranging between about 50  $\mu$ s and 1 ms, with a few hundred  $\mu$ s being a typical duration [*Briggs et al.*, 2010; *Fishman et al.*, 2011]. Events longer than a few ms may likely be terrestrial electron beams (TEBs), generated by TGFs near one foot point of the geomagnetic field line that passes through the spacecraft [*Dwyer et al.*, 2008a; *Briggs et al.*, 2011].

<sup>1</sup>Department of Physics and Space Sciences, Florida Institute of Technology, Melbourne, Florida, USA.

<sup>2</sup>Department of Electrical and Computer Engineering, University of Florida, Gainesville, Florida, USA.

Corresponding author: J. Dwyer, Department of Physics and Space Sciences, Florida Institute of Technology, Melbourne, FL 32901, USA. (jdwyer@fit.edu)

[4] To date, over a thousand terrestrial gamma-ray flashes (TGFs) have been detected by spacecraft in low-earth orbit (e.g., see [http://scipp.ucsc.edu/~dsmith/tgflib\\_public](http://scipp.ucsc.edu/~dsmith/tgflib_public) for a partial list). In addition to a ground level flash observed in 2003 [Dwyer et al., 2004a] (see Section 1.2), before this work, only one other TGF has been observed from within our atmosphere. That event was measured by the ADELE instrument onboard a NCAR/NSF G-V aircraft at an altitude of 14.1 km, approximately 10 km away from the TGF source within a thundercloud near the Florida/Georgia border [Smith et al., 2011]. Even though the event was relatively close to the aircraft, 10 km compared to 600 km for spacecraft, at the 14.1 km altitude there was enough air between the TGF and the aircraft to attenuate the gamma-rays so that the number of photons measured was about the same as from space.

[5] It is amazing that such a spectacular natural phenomenon, seen so frequently from space, has been directly measured so few times from within our atmosphere. Based upon the rate of TGFs from spacecraft observations, TGFs may occur once per thunderstorm, on average, so they are by no means rare [Østgaard et al., 2012]. They are also of practical interest, since the fluence of high energy electrons and gamma-rays is large enough that if an aircraft were directly struck by a TGF, the radiation dose to individuals inside could be significant [Dwyer et al., 2010; Kutsyk et al., 2011].

[6] In this paper, we report the new observations of a second TGF-like ground level gamma-ray flash, observed on June 30, 2009 at the ICLRT. This event gives new insight into the mechanisms that may be responsible for generating TGFs.

## 1.2. The 2003 Ground Level TGF

[7] In order to understand the new gamma-ray flash observation described in this paper, it is useful to first review the one previously observed ground level TGF and compare its properties to those of typical x-ray emission from lightning.

[8] Just prior to the RHESSI TGF observations, Dwyer et al. [2004a] reported the observation of an intense gamma-ray flash on the ground at sea level on 15 August 2003, produced in association with the initial-stage of rocket-triggered lightning at the UF/Florida Tech International Center for Lightning Research and Testing (ICLRT) at Camp Blanding, FL. The flash, referred to hereafter as the 2003 gamma-ray flash, was observed simultaneously on three NaI(Tl)/photomultiplier tube (PMT) detectors that were located 650 m from the triggered lightning channel and exhibited gamma-ray energies extending up to 11 MeV. It consisted of 227 individual gamma-rays (measure on one of the NaI/PMTs) that arrived over a 300  $\mu$ s time period in coincidence with an 11 kA current pulse through the lightning channel to ground. The flash of gamma-rays had very different characteristics from the x-ray emissions frequently seen in association with the dart leaders, dart stepped leaders, chaotic leaders, and stepped leaders during triggered lightning and natural lightning [Dwyer et al., 2003, 2004b, 2005; Hill et al., 2012]. In particular, the energy spectrum of the 2003 gamma-ray flash was much harder, extending to much higher energies than the x-ray emissions from lightning. For example, Dwyer et al. [2004b] used NaI/PMT detectors with varying amounts of bronze attenuators over the scintillators to infer that several triggered lightning dart leaders produced x-rays only up to about 250 keV. Dwyer

et al. [2005] measured a natural lightning strike at the ICLRT and found that the x-rays appeared to have energies that were similar to those of triggered lightning. Later, Saleh et al. [2009], using the Thunderstorm Energetic Radiation Array (TERA) at the ICLRT, found that one dart step leader had an energy spectrum with a characteristic energy of about 1 MeV. Using a “pinhole” aperture x-ray camera, Dwyer et al. [2011] presented x-ray images of two chaotic leaders from rocket triggered lightning, showing that most of the x-ray emission came from the region near the leader tip and had energies below about 400 keV.

[9] A second difference between the 2003 gamma-ray flash and x-rays from lightning is the x-rays from lightning are almost always observed to arrive in intense sub-microsecond bursts [Dwyer et al., 2004b]. It has been shown that these bursts occur during the step formation of stepped leaders and dart-stepped leaders [Dwyer et al., 2005; Howard et al., 2008] and so are connected to the propagation of lightning leaders. All of the individual pulses measured during the 300  $\mu$ s gamma-ray flash had pulse shapes consistent with individual photons and showed no evidence of the kind of pulse pile up seen in association with lightning leaders.

[10] Finally, most of the x-rays seen from lightning occur when the lightning leader is within a several hundred meters of the ground [Saleh et al., 2009]. Often, pulses are seen in the electric and magnetic fields and their derivatives and large deflections are seen in the vertical electric field as the leader approaches the ground (see Figures 7 and 1 for examples of the former and the latter, respectively). No such signatures were seen during the 2003 gamma-ray flash. Indeed, the timing of that event observed on the ground, 40 ms after the beginning of the triggered lightning initial-stage, suggests that it was associated with processes within the cloud, kilometers above the ground. This observation led Dwyer et al. [2004a] to suggest that the ground level gamma-ray flash originated from within the overhead thundercloud. They also suggested that similar gamma-ray flashes that originate from thunderclouds might have been observed from space in the form of TGFs, a hypothesis that was later confirmed by RHESSI.

[11] TGFs and the 2003 ground level flash reported by Dwyer et al. [2004a] have several similarities, including similar energy spectra, similar durations, both associated with lightning and apparently both originating from thunderclouds; with the differences being the ground level event likely originated lower in the cloud, was directed downward, and was initiated by a triggered lightning event rather than natural intracloud lightning.

## 1.3. Source Mechanisms

[12] Additional insight comes from the source mechanisms involved in producing the x-rays and gamma-rays in the atmosphere. It is generally accepted that TGFs involve relativistic runaway electron avalanche (RREA) production [Gurevich et al., 1992; Lehtinen et al., 1999; Gurevich and Zybin, 2001; Dwyer, 2003; Dwyer and Smith, 2005]. On the other hand, Dwyer [2004] showed that the x-rays from lightning leaders are not generated by the RREA mechanism, since the observed x-ray flux was too large and the observed x-ray energy spectrum was too soft to be consistent with the RREA mechanism. Instead, Dwyer [2004] proposed

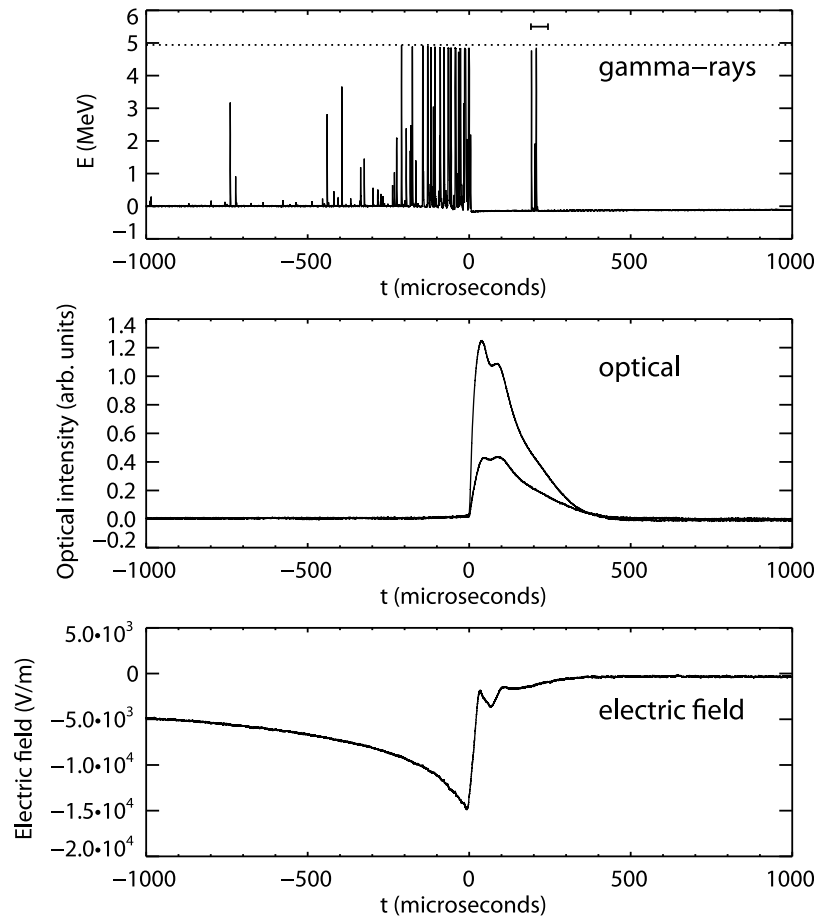


**Figure 1.** (top) X-ray and gamma-ray emissions measured by station T-8 from the June 30, 2009 natural -CG lightning. The start of the return stroke is at  $t = 0$ . The emissions before the return stroke are x-rays from the lightning leaders. The burst starting at about  $200 \mu\text{s}$  is the gamma-ray flash. The horizontal dotted line shows where the signals are clipped due to saturation of the fiber optic electronics. The small horizontal bar shows the duration of the gamma-ray flash on all detectors. (middle) Optical emission from the return stroke measured by the northeast optical (NEO) facing southwest, and the southwest optical (SWO), facing northeast. The largest trace is from SWO. (bottom) Vertical electric field measured at station E-10. The negative deflection of the field, seen on the left side of the plot, is due to the stepped leader lowering negative charge to the ground.

that cold runaway electron production in high fields is responsible for the emissions [Gurevich, 1961; Moss *et al.*, 2006]. It is possible that the energetic electrons produced by lightning leaders undergo additional RREA multiplication to produce the bright TGFs [Dwyer, 2008; Saleh *et al.*, 2009; Carlson *et al.*, 2010; Dwyer *et al.*, 2010; Celestin and Pasko, 2011, 2012]. Alternatively, a positive feedback effect caused by backward propagating positrons and backscattered x-rays, called relativistic feedback, could seed RREAs generating a TGF [Dwyer, 2003, 2005, 2007, 2008, 2012]. Regardless of the exact model, an important distinction is that all viable TGF models involve RREAs, and x-rays from lightning, at least observed to date, do not. Furthermore, any intense burst of gamma-rays in our atmosphere with energies exceeding 7 MeV, the characteristic RREA energy scale, almost certainly is produced by runaway electrons experiencing RREA multiplication. Consequently, the fact that the 2003 ground

level flash had energies exceeding 10 MeV implies that it also shared the same RREA source mechanism with terrestrial gamma-ray flashes.

## 2. Instrumentation

[13] The University of Florida/Florida Tech International Center for Lightning Research and Testing (ICLRT) at Camp Blanding, FL, is a  $\sim 1 \text{ km}^2$  facility located in north central Florida between Gainesville and Jacksonville. It is well instrumented for measuring both natural and rocket-and-wire triggered lightning. One set of instruments at the ICLRT is the Thunderstorm Energetic Radiation Array (TERA), designed to measure energetic radiation (x-rays, gamma rays and energetic charged particles) from thunderclouds, lightning and cosmic ray extensive air showers (EASs). The TERA instruments are distributed at different

stations across the  $\sim 1 \text{ km}^2$  ICLRT site (see Figures 4 and 5). TERA is also part of an experiment called the MSE (Multiple Station Experiment). Besides the x-ray detectors, the MSE/TERA stations are equipped with instrumentation to measure electric fields and their derivatives as well as magnetic fields using flat plate antennas and loop antennas [Jerould, 2007].

[14] At the time of the June 30, 2009 observations, 19 TERA stations were operating, composed of twenty-three  $7.6 \text{ cm} \times 7.6 \text{ cm}$  cylindrical NaI(Tl)/Photomultiplier tube (PMT) detectors and two  $7.6 \text{ cm} \times 7.6 \text{ cm}$  cylindrical LaBr<sub>3</sub>(Ce)/PMT detectors. Each of the TERA instruments is contained in a  $1/8''$  (0.32 cm) thick aluminum box to shield the instrument from moisture and light [Dwyer *et al.*, 2008b; Saleh *et al.*, 2009]. The aluminum box lids allowed x-rays with energies down to about 30 keV to enter from all directions, while acting as a Faraday cage to shield the instruments from external static electric fields and RF noise. Six of these twenty five detectors were also enclosed in 0.32 cm thick lead attenuators. These lead attenuators absorb x-rays below  $\sim 300 \text{ keV}$ , thereby helping determine the energy spectrum by comparing the signals from the unattenuated (with 30 keV cut-offs from the Al lids) and the attenuated detectors. In addition, seven of the stations had detectors made of  $1 \text{ m}^2$  by 2 cm-thick plastic (BC-408, Pilot F) scintillators. The scintillators are shielded inside two (0.32 cm thick) aluminum light tight boxes and viewed by two PMT detectors. These plastic detectors, which were designed to primarily measure cosmic ray air showers, also have sensitivity to x-ray and gamma-rays, but unlike the inorganic (NaI and LaBr<sub>3</sub>) scintillators they have poor energy resolution.

[15] All detectors, with the exception of the LaBr<sub>3</sub> detectors, were powered by internal 12 V batteries, and Opticom FM (68 k-ohm input impedance, 30 MHz bandwidth) analog fiber optic links were used to transmit the signals from the PMT anodes directly to the data acquisition system located in a separate, shielded trailer. The LaBr<sub>3</sub> detectors were powered directly from and had signals sent directly to a shielded trailer. All the fiber optic delays have been accurately measured from end to end, and these delays were used in the analysis to align the signals in time from different stations [Howard *et al.*, 2008].

[16] The data acquisition system is triggered when the incident current measured from triggered lightning exceeds a threshold of 6 kA, or when two optical sensors, located at the northeast and southwest corners of the site, are simultaneously triggered due to nearby natural lightning. The natural flash reported here was triggered by the two optical sensors.

[17] Signals from all x-ray detectors and the MSE are recorded by Yokogawa ScopeCorders, with 12 bit resolution and a sampling rate of 10 MHz. The scope's records have lengths of either 2 s of data with 1 s of pre-trigger sampling or 1.6 s of data with 0.8 s of pre-trigger sampling. A subset of eight detectors from TERA, along with MSE instruments, called the time-of-arrival (TOA) network, are recorded using LeCroy Waverunner scopes that sampled at 250 MHz with 8 bit resolution, with a total record length of 2 ms and 1 ms of pre-trigger sampling, allowing faster timing to help determine the location of the source of x-ray emissions and electric field changes.

[18] A Cs-137 662 keV radioactive gamma-ray source was used to calibrate the energy scale of the NaI and LaBr<sub>3</sub> scintillation detectors. We note that 3 detectors did not have accurate energy calibrations at the time of the observations. For these detectors, the calibration factor was found by comparing nearby detectors with known calibrations using the x-rays from the lightning leader.

### 3. Observations

[19] On the morning of June 30, 2009 a very strong band of rain and thunderstorms came out of the Gulf of Mexico and moved over land toward the ICLRT. The storm produced large quantities of rain, but produced little lightning. That morning, a large (99.4 kA NLDN peak current) natural lightning flash was visually observed to strike toward the eastern side of the ICLRT. The CG-lightning, which was a negative, downward propagating, single stroke flash, triggered data acquisition from instruments at the ICLRT. Unfortunately, the GPS time card stamping program was locked up and did not record the exact trigger time. The scope times recorded on the acquisition files indicate the trigger time was around 7:21 A.M. EST (11:21 UT). NLDN recorded a negative CG lightning at 11:21:29.496 UTC whose ground strike point was located about 800 m to the northeast of the ICLRT (nominal error of a few hundred meters) with a peak current of 99.4 kA.

[20] The largest electric field changes were recorded at the two stations on the far eastern side of the ICLRT. The optical sensor located on the southwest corner of the ICLRT (SWO), pointed toward the northeast, saw almost four times the optical intensity as the optical sensor located at northeast corner of the ICLRT (NEO), pointed toward the southwest (see Figures 1, 4, and 5). The x-ray production from this flash was very strong, with large x-ray pulses records on all TERA stations over the entire  $1 \text{ km}^2$  facility. The x-ray pulses were recorded starting roughly 2 ms before the return stroke, building in intensity until the time of the return stroke at which point the x-rays pulses decreased dramatically, as is typical with all natural and triggered lightning observed so far. Also, as is common for natural lightning, a few small x-ray pulses were recorded up to 13  $\mu\text{s}$  after the start of the return stroke, possibly from other branches that were not involved in the attachment to ground and so continued to propagate for a short time. The NaI detectors on the eastern portion of the site measured the largest signals, recording saturated pulses for more than 200  $\mu\text{s}$  prior to the return stroke. Using the arrival times of the x-ray pulses, we identified at least two distinct x-ray emitting branches located toward the east of TERA. One branch appears to be located approximately over the detectors in the northeastern corner of the ICLRT. Another branch appears to be somewhere to the northeast of NE optical. Presumably one of these branches attached to ground to form the return stroke. Altogether, these data show that the strike terminated off the eastern edge of the site, with multiple branches present. This is consistent with the NLDN location of the ground contact point (lat = 29.9472 and lon = -82.0211), which is about 800 m to the northeast of NE optical.

[21] The June 30, 2009 flash had one particular feature that was very unique. Unlike all other natural and rocket-triggered lightning strokes recorded at the ICLRT, a separate

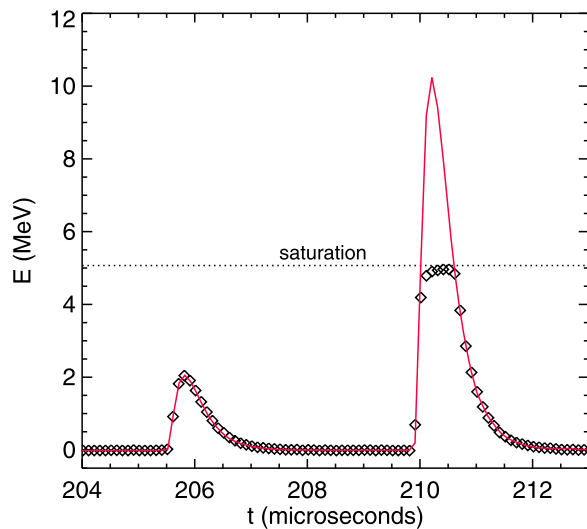


**Figure 2.** Waveforms from two gamma-rays detected by the NaI/PMT at station T-8 during the gamma-ray flash (black diamonds). The red curves are the fits of the detector response function. The pulse height of the response function gives the gamma-ray energy. The start of the return stroke is at  $t = 0$ . The horizontal dotted line shows where the signals are clipped due to saturation of the fiber optic electronics.

flash of gamma-rays was recorded after the return stroke commenced. The gamma-ray flash lasted  $52.7 \mu\text{s}$  (time between the first and last photons), and started  $191 \mu\text{s}$  after the initiation of the stroke,  $178 \mu\text{s}$  after all x-ray emission from the stepped leaders terminated. A total of 19 gamma-ray photons were recorded on 9 TERA NaI detectors and 2 plastic scintillators, with energies ranging from 64 keV to over 20 MeV.

[22] Figure 1 shows the waveform from one NaI detector (T-8) along with optical emissions recorded by the northeast optical (NEO) and southwest optical (SWO) photodiodes and the electric field recorded by a flat plate antenna (E-10). The start of the return stroke, as defined by the beginning of the optical emission, occurs at  $t = 0$ . The x-ray emission before  $t = 0$  are the usual x-rays from the lightning leaders [e.g., Dwyer *et al.*, 2005]. The vertical scale is in MeV and shows the approximate deposited energy in the detector. By comparing the x-ray pulses to the detector response functions, it can be seen that the x-rays from lightning leaders are piling up, with many overlapping x-ray pulses arriving over a very short time period. This results in much larger pulse sizes than the energies of the individual photons. Therefore, great care must be taken not to overestimate the maximum energy of the photons. The pulses on this detector also saturate the electronics over the last  $220 \mu\text{s}$  before the return stroke.

[23] The gamma-ray flash can be seen starting at  $t = 192 \mu\text{s}$ . Unlike the x-rays from the lightning leaders, the pulses in the gamma-ray flash show no sign of pulse pile up and so the energies seen in Figure 1 better represent the true energies of the individual gamma-ray photons. Note that we are assuming that the measured energetic radiation is composed of photons. However, it cannot be ruled out that some of the pulses were actually energetic electrons or positrons (see below).

[24] The lack of pulse pile up in this data after the start of the return stroke may be demonstrated in three ways: First, all pulses were fit with the detector response functions and found to be consistent with single photons. The detector response, which arises from the effects of the NaI light decay time ( $\sim 0.23 \mu\text{s}$ ) and the front end electronics, is found for each detector by using background pulses (from background energetic radiation) at times well separated from the lightning. Figure 2 is a segment of data from Figure 1 during the gamma-ray flash, showing two gamma-ray pulses (black diamonds) along with the fit of the detector single photon response function (red curves). As can be seen, both pulses are well fit with the response function and are consistent with single photons. The second pulse is clipped by the fiber optic transmitter/receiver electronics at 1 V (dotted line). Even though the peak of the pulse was not recorded, the energy is still found by the fit of the response function.

[25] The average counts on all the inorganic detectors was found to be 0.68 pulses per detector, distributed over a duration of  $52.7 \mu\text{s}$ . Therefore, the probability that two photons would arrive at the same time (within  $<0.1 \mu\text{s}$  to remain consistent with the pulse fitting) on a single detector is very small. In one particular TERA instrument a  $>20 \text{ MeV}$  pulse was recorded on the un-attenuated detector, while none were recorded at that time on the other (attenuated) detector in the same box, less than 0.5 m away. If the pulse was composed of multiple x-rays in the hundred keV range, as is typical of lightning leader emission, then it is very unlikely that several tens of photons would be recorded on one detector and none on the other.

[26] Finally, the actual arrival time of each pulse is measured and found to be consistent with the photons arriving approximately uniformly in time with no evidence for small time scale grouping of the photons. Specifically, by considering the 12 photons that arrive within the first  $25 \mu\text{s}$  of the gamma-ray flash, the most intense part, it was found that the distribution of arrival times is consistent with a uniform random distribution. For the remaining pulses that follow, the odds of two or more arriving at nearly the same time are even less likely.

[27] The background rate on the detectors was recorded during the 1.6 to 2 s records and found to be about  $150 \text{ s}^{-1}$  above 50 keV for the un-attenuated detectors and about half that value for the attenuated detectors. Above 1 MeV the background rate was about  $7 \text{ s}^{-1}$  on each detector. As a result, the probability that even one pulse,  $>50 \text{ keV}$ , during the gamma-ray flash was due to background was 0.17. The probability that one pulse,  $>1 \text{ MeV}$ , during the gamma-ray flash was due to background was 0.01. The probability that the entire gamma-ray flash was produced by a fluctuation in the background is less than  $10^{-22}$ . As a result, we can rule out background count fluctuations as being the source of the gamma-ray flash. Furthermore, the electronic noise on the detectors was typically below the 50 keV level. Because each pulse was fit with the detector response function, which has a shape very different from most noise fluctuations, electronic noise can be ruled out as well.

[28] The pulses in the gamma-ray flash were individually fit with a detector response functions and the peak pulse amplitudes were found, as seen in Figure 2. The Cs-137 calibration data were then used to calculate the energies of the pulses, which following the discussion above, are the

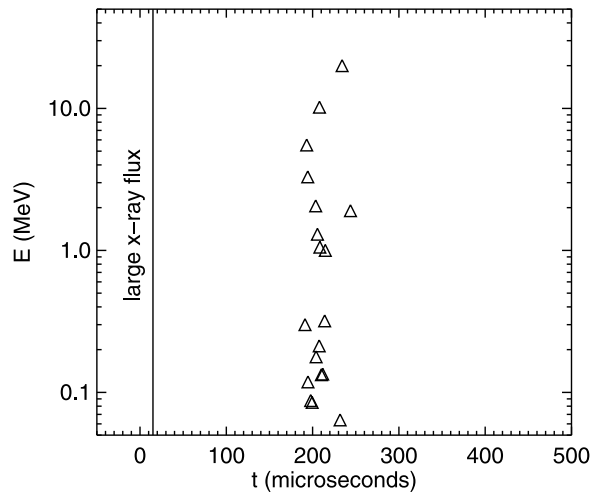


**Figure 3.** Measured gamma-ray energies versus time. The start of the return stroke is at  $t = 0$ . The x-rays from the lightning leader are all on the left side of the vertical solid line.

energies of individual gamma-ray photons that compose the gamma-ray flash. The NaI and LaBr<sub>3</sub> detectors have been tested with multiple radioactive sources and are found to have linear responses over the energy range tested, up to 1.3 MeV. Above that energy, it is assumed that the detector responses remain linear, proportional to deposited energies in the scintillators. Any nonlinearity that does occur would likely reduce the pulse size and so would result in the photon energies being underestimated. With this in mind, the largest pulse recorded was compared with pulses produced by cosmic ray muons. Calculations of the ionization energy loss rate of minimum ionizing muons traversing the 7.3 cm thick NaI scintillator show that they deposit at least 33 MeV in the crystal, with more energetic and inclined muons depositing more energy. By fitting the cosmic ray muon pulses to the large gamma-ray pulse, and using 33 MeV per muon, we find that the gamma-ray deposited at least 20 MeV in the detector. Since the muon deposited energy was a lower limit, the 20 MeV photon energy is also a lower limit, although to be conservative we shall label it simply as 20 MeV.

[29] A scatterplot of the individual photon energies and their arrival times at the detectors is shown in Figure 3. As can be seen, there are no background counts above 50 keV in this 500  $\mu$ s time window. Before  $t = 13 \mu$ s, a large number of pulses occur in association with the lightning leaders and are not shown. These gamma-ray data appear very similar, both in duration and energy spectra, to recent Fermi/GBM of TGF data [Briggs *et al.*, 2010].

[30] The average count rate of gamma-rays  $>1$  MeV striking TERA for the 53  $\mu$ s flash was  $(5.3 \pm 2) \times 10^3$  s<sup>-1</sup> per detector, which is about 760 times the local background rate. For comparison, the average count rate for the 2003 gamma-ray flash was  $7.6 \times 10^5$  s<sup>-1</sup> per detector, 140 times larger than the flash under discussion. If we use the geometric area of the detectors ( $4.57 \times 10^{-3}$  m<sup>2</sup>) as the effective area of detection (assuming the detection efficiency is 1 for these energies), then the average flux of gamma-rays  $>1$  MeV [photons/s m<sup>2</sup>] was  $(1.2 \pm 0.5) \times 10^6$  s<sup>-1</sup> m<sup>-2</sup> and the

average fluence [photons/m<sup>2</sup>] was  $61 \pm 20$  m<sup>-2</sup>. Taking into account the reduced efficiency of the attenuated detectors, the average flux and fluence of gamma-rays  $>50$  keV near the ground was  $(3.5 \pm 0.8) \times 10^6$  s<sup>-1</sup> m<sup>-2</sup> and  $180 \pm 40$  m<sup>-2</sup>, respectively.

[31] Because TERA consists of 19 stations distributed over the 1 km<sup>2</sup> ICLRT site, spatial information about the gamma-rays can also be determined. Figure 4 shows a map of the ICLRT site along with the gamma-ray flash data. The crosses show the locations of all the detectors. (The offsets of detectors at the same station are exaggerated for clarity.) The red circles show the energies of the individual photons measured at each detector, with the larger circles having higher energies. For clarity, at each station, when multiple photons were recorded, the circles are plotted with slight offsets so that they may be seen more clearly. The two plastic scintillators that recorded pulses are shown as striped red circles. For these two detectors the energies are rough estimates. From the plot, it can be seen that the emission is both recorded over a large area at the ICLRT and is non-uniform. Indeed, the detector on the lower right (T-8) recorded 5 photons, while many others recorded none.

[32] For comparison, we next plot the x-ray data from the lightning leaders that preceded the gamma-ray flash. To do this, the detector pulse heights from all of the NaI detectors were measured from  $t = -2000 \mu$ s to  $t = -500 \mu$ s before the

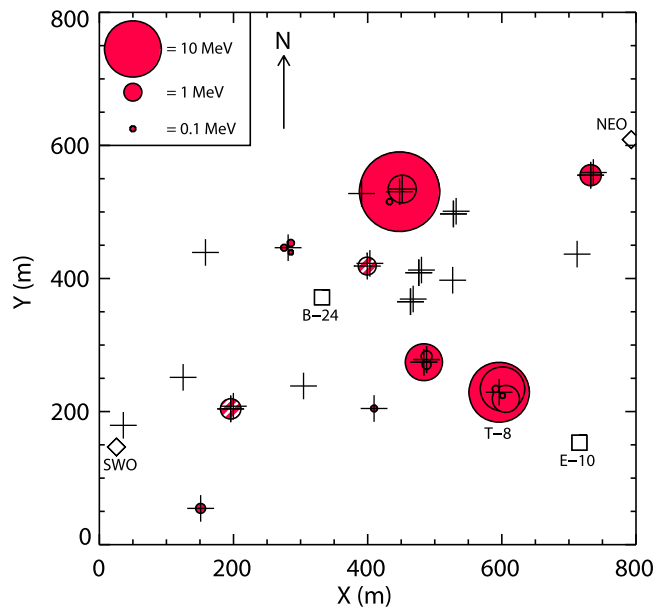


**Figure 4.** Spatial distribution of the gamma-ray flash measured on the ground at the ICLRT. The diagram shows the locations of all the TERA detectors (crosses), northeast optical (NEO), southwest optical (SWO), and stations E-10 and B-24. Each solid red circle shows the detection of an individual gamma-ray on a NaI/PMT detector with the area proportional to the energy. The striped red circles show the deposited energy on the plastic scintillators. For clarity, multiple circles on the same detectors are given slight offset when plotted. Also, the separation for detectors at the same stations are exaggerated for clarity.

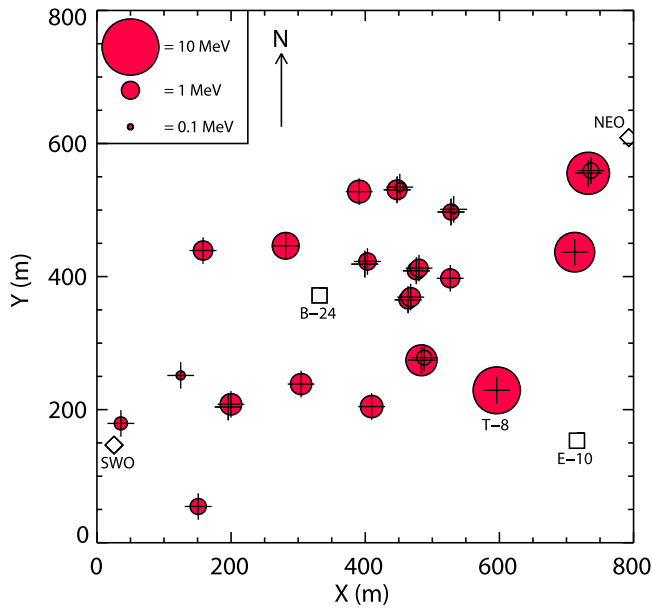


**Figure 5.** Spatial distribution of the x-rays from the lightning leaders ( $-2000 \mu\text{s}$  to  $-500 \mu\text{s}$ ) measured on the ground at the ICLRT. The diagram shows the locations of all the TERA detectors (crosses), northeast optical (NEO), southwest optical (SWO), and stations E-10 and B-24. Each solid red circle shows the total deposited energy on each detector with the area proportional to the energy. The plastic detectors are not shown. For clarity, the circles for detectors at the same stations are offset slightly.

return stroke. Later times were either too heavily saturated or piled up to make reliable photon energy measurements. Even during this earlier time, some of the larger pulses show clear signs of being composed of multiple photons, with pulse widths wider than the detector response function and simultaneous pulses being recorded on multiple detectors.

[33] The spatial distribution of these x-ray energies recorded from the lightning leader is shown in Figure 5. Note that Figure 5 shows the total deposited energy in each detector (only the NaI and the LaBr<sub>3</sub> detectors are shown), whereas Figure 4 shows the energies of each of the recorded photons. As can be seen, the most intense x-ray emission is recorded on the eastern side of the ICLRT, near the inferred lightning strike point. However, substantial emission is also seen over the rest of the site. During this time period ( $t < -500 \mu\text{s}$ ), the leaders were probably several hundred meters to a couple of kilometers above the ground, resulting in a more uniform distribution than occurs just before the lightning attaches to the ground (see *Saleh et al.* [2009] for more details).

[34] Although perhaps not immediately apparent to the eye, Figures 4 and 5 have some common features that are statistically significant: Both figures generally show more energetic radiation on the southernmost and northernmost detectors with more radiation recorded on the eastern side of the site. In the next section, we shall perform a detailed statistical analysis and show that the gamma-ray flash data and the lightning leader data, seen in Figures 4 and 5, in fact, are consistent with arising from the same spatial source

distribution. However, in Section 4.2, we will also show the electrical properties of and the resulting characteristics of the high energy radiation emitted from the same region at different times are very different.

## 4. Analysis

### 4.1. Spatial Distribution of the Source

[35] In this section, we shall compare the spatial distribution seen in Figure 4 with several source distribution models, thus providing information about the location(s) of the gamma-ray source. Specifically, we shall consider three models for the gamma-ray source: First, we shall consider a gamma-ray source that is located very high above the ground, e.g., from within the overhead thundercloud, or is very broadly distributed, resulting in an approximately uniform distribution of gamma-rays at the ground at the ICLRT. Next, we shall consider a single compact source region at an intermediate height ( $< \text{few km}$ ) sending a downward beam of gamma-ray toward the ground. Finally, we consider a model in which the lightning leader emission and the gamma-ray emission have the same spatial source distribution, i.e., the source regions are the same for both.

[36] Monte Carlo simulations show that the gamma-ray distributions on the ground for both the high altitude and intermediate altitude cases may be approximated by a model of the form

$$f(x, y) = f_0 e^{-\sqrt{(x-x_0)^2 + (y-y_0)^2} / \lambda}, \quad (1)$$

where  $f$  gives the gamma-ray fluence on the ground as function of positions,  $x$  and  $y$ , and  $x_0$  and  $y_0$  are the coordinates of the foot point on the ground directly below the overhead source. This form is justified by detailed Monte Carlo simulations of RREAs and the accompanying gamma-ray emissions and photon propagation [Dwyer, 2007]. For vertical electric fields, the horizontal attenuation length  $\lambda$  is found to range from about 100 m to hundreds of meters, increasing with the source altitude. At several kilometers,  $\lambda$  is large, and equation (1) becomes approximately a uniform distribution over a region the size of the ICLRT. Interestingly, it is found that the horizontal attenuation length  $\lambda$  depends only weakly upon the photon's energy, in contrast to the TGFs observed from space, which show a substantial change in energy spectrum with increased lateral distance from the TGF source. For TGFs seen in space this is due to the fact that Compton scattered photons, which have lower energies, dominate at larger angles outside the primary TGF gamma-ray beam [Hazelton et al., 2009]. For the case of gamma-rays propagating near the ground, the low energy Compton scattered photons do not travel far through the air (and have no opportunity to escape to space) and so are produced locally from the more energetic photons. It is also found from Monte Carlo simulations that a downward beam of energetic positrons, as might be produced by relativistic feedback for upward directed RREAs, also generates gamma-rays with a distribution described by equation (1). Because the average energy of the positrons is higher than the runaway electrons [Dwyer, 2012], for the same source altitude, the positrons tend to produce a slightly tighter beam on the ground with a smaller  $\lambda$  than the runaway electrons.

[37] To test the source distribution models of the gamma-ray flash, we construct the likelihood function from the product of the Poisson distributions for the  $N$  detectors:

$$L = \prod_{i=1}^N \frac{f_i^{n_i} e^{-f_i}}{n_i!}, \quad (2)$$

where  $f_i$  is the model prediction for the number of counts recorded on the  $i$ th detector and  $n_i$  is the actual number of counts recorded. For this part of the analysis, we exclude the two plastic scintillators, since it is difficult to estimate their effective areas for this event. On the other hand, the two LaBr<sub>3</sub> detectors have about the same effective areas as the NaI detectors and so they are included, making the total number of detectors used  $N = 25$ . There were 17 photons detected for this subset of detectors. For a given set of observations,  $n_i$ , the best estimate of each  $f_i$ , written as  $\hat{f}_i$ , is found by finding the maximum of the likelihood function,  $L$ . If the  $\hat{f}_i$ 's are functions of additional parameters (e.g.,  $x_o$ ,  $y_o$  and  $\lambda$  in equation (1)), equation (2) may be maximized with respect to those parameters to find their most likely values. Following *Hauschild and Jentschel* [2001], once the values of the  $\hat{f}_i$  are found using the maximum likelihood technique, the confidence in the model, i.e., the goodness of fit, is tested by calculating the Pearson's  $\chi^2_P$  statistic

$$\chi^2_P = \sum_{i=1}^N \frac{(n_i - \hat{f}_i)^2}{\hat{f}_i}. \quad (3)$$

The value of  $\chi^2_P$  is then compared to the  $\chi^2$  distribution to calculate the probability (P-value) that  $\chi^2 > \chi^2_P$  for the number of degrees of freedom. Note that the maximum of the likelihood function (equation (2)) is used rather than the minimum of the  $\chi^2_P$  (equation (3)) because the latter overestimates the means, i.e., it is an inconsistent estimator. On the other hand, the  $\chi^2_P$  is better for calculating the goodness of fit since, unlike  $\chi^2$  statistics based upon the likelihood function, it has an expectation value equal to the number of degrees of freedom,  $\nu$ , for all values of the true mean number of counts, i.e.,  $\langle \chi^2 \rangle / \nu = 1$  [*Mighell*, 1999].

[38] Because the data are sparse with a small number of counts and many zero counts, one may question the validity of using the  $\chi^2$  distribution, which describes the  $\chi^2_P$  statistic only when the number of counts is large [*Evans and Rosenthal*, 2004]. In our case, we are working with just 17 photons, so further binning the data offers little help. To augment the goodness of fit test, we calculate the  $\chi^2_P$  distribution numerically using a Monte Carlo method [*Boyle et al.*, 1997; *Humphrey et al.*, 2009]. Assuming that the estimations,  $\hat{f}_i$ , are close to the true values, we calculate a large set of simulated data,  $n_i$ , that follows Poisson distributions with means  $\hat{f}_i$ . For each sample of the simulated data, a new estimation (best fit) of  $f_i$  are found using equation (2). We then calculate  $\chi^2_P$  according to equation (3), using the simulated data and their best fit models, thus producing a distribution of  $\chi^2_P$  values. The  $\chi^2_P$  calculated from the measured data is then compared to this distribution and the P-value is found. Specifically, the fraction of  $\chi^2_P$  values, calculated from the simulated data, that are larger than the measured value gives an estimate of the significance in which the model may

be rejected. For instance, a probability (P-value) greater than about 0.05 (and less than 0.95) gives us confidence that the model is a good fit and is indeed correct. Values less than this exclude the model with a significance given by the probability.

[39] Let us first test the hypothesis that the gamma-ray flash counts are produced by a uniform spatial source distribution, for instance, corresponding to a high altitude source. If the detection efficiency were the same on all detectors then  $f_i = f_o = \text{constant}$  for all  $i$ . However, six detectors were attenuated with lead, blocking photons below about 300 keV. Measurements from the un-attenuated detectors show that about 50% of the photons in the gamma-ray flash arrive with energies below 300 keV. To account for this, the expected number of counts predicted by the model is reduced by 0.5 for the attenuated detectors. In addition, four of the un-attenuated detectors had smaller signal-to-noise ratios (either due to lower gains or faster sampling rates), only allowing photons with energies greater than about 200 keV to be measured. For simplicity, the expected number of counts predicted by the model is reduced by 0.5 for these detectors as well. The maximum likelihood solution is then found to be  $\hat{f}_i = 0.84$  counts/detector for the un-attenuated detectors (normal signal to noise) and half that for the attenuated and low-signal-to-noise detectors. For the gamma-ray flash it is found that the probability that the data came from a uniform spatial distribution is  $P = 0.0070$ , allowing us to exclude a uniform distribution with high significance. This fact was implied above when we discussed that one detector had 5 counts while many had none. This result has the immediate implication that the source cannot come from an altitude of more than a few kilometers, since the higher the source altitude, the more uniform the spatial distribution. If instead, we relied on the  $\chi^2$  distribution, we find that  $P = 0.0028$ , also excluding the model with high significance.

[40] The maximum likelihood fit of equation (1) to the gamma-ray flash data gives, in the coordinate system plotted in Figures 4 and 5,  $x_o = 595$  m (+66 m, -54 m),  $y_o = 203$  m (+47 m, -194 m),  $\lambda = 189$  m (+100 m, -50 m), centered near the detector (T-8) with the largest number of counts. Here, the errors are the ( $1\sigma$ ) confidence intervals calculated from the likelihood function (equation (2)). This  $\lambda$  is consistent with a RREA source altitude of roughly 2 km. For this fit,  $\chi^2_P = 40.1$  with 21 degrees of freedom. Using the  $\chi^2$  distribution we find that  $P = 0.007$ , which is slightly larger than the P-value found from the  $\chi^2$  distribution for the uniform source function. However, this probability is still small enough that we can exclude this single source location model as well. In other words, the ground level gamma-ray flash is not consistent with a single runaway electron or positron source at any altitude or location, with high altitudes being less likely.

[41] Finally, using the data for the lightning leaders shown in Figure 5 as our model for the gamma-ray flash emission (Figure 4), we find that  $\chi^2_P = 29.4$  with 24 degrees of freedom. Calculating the P-value numerically, we find that the gamma-ray flash data agrees with the model with a probability  $P = 0.21$ . Instead, using the  $\chi^2$  distribution we find that  $P = 0.20$ . In other words, the gamma-ray flash data is statistically consistent with having originated with a same spatial

distribution as the lightning leader x-ray data. As a check, the x-ray leader data were randomly exchanged (1000 times) among detectors and it was found that the true arrangement was in the top 0.4% of all P-values.

[42] Rather than treating the leader x-rays as the model and the gamma-ray flash as the data, it is more reasonable to treat both sets as data and ask whether both sets are consistent with arising from the same parent distribution (albeit with different average fluxes). For this model, all of the  $f_i$  are independent and there is an additional normalization factor that accounts for the different total number of x-ray leader photons and gamma-ray flash photons. Because the x-rays from the leaders have a softer energy spectra than the gamma-ray flash, the counts at low energies are affected more by the attenuators (and the low signal to noise detectors) than for the gamma-ray flash. To correct for this, only the un-attenuated detectors with normal signal-to-noise ratios are used for the x-ray data. For this calculation, the number of photons must be estimated for the x-ray leader data. Following *Dwyer et al.* [2011], we conservatively assign the average photon energy of 150 keV and divide the deposited energy by this average energy to get an estimate of the number of x-ray photons recorded in each detector, thus allowing Poisson errors to be assigned to the energy data. For the goodness of fit test, this average energy is a conservative choice, since it is smaller than the 350 keV average energy of all the measured pulses, and smaller values give larger estimates of the number of photons and hence smaller error bars, worsening the goodness of fit.

[43] We first did the maximum likelihood fits for the combined x-ray leader and gamma-ray flash data sets and then found that  $\chi^2_P = 26.0$  with 23 degrees of freedom. The Monte Carlo  $\chi^2_P$  calculation then gives a probability  $P = 0.33$ . Using the  $\chi^2$  distribution gives  $P = 0.30$ . In other words, both data sets are statistically consistent with arising from the same source locations, i.e., the lightning leaders. Again, randomly shuffling the x-ray measurements (1000 times) among the 25 detectors shows that most other arrangements give much worse agreements, with the true configuration having a P-value in the top 0.5% of all P-values. Also, uniformly distributing the same number of x-ray leader counts produces a poor fit. As a final test, we found that the results did not change when we removed any one of the detectors from the analysis, making sure that the good agreement was not arising from any single detector. Thus, we can state with confidence that the x-ray leader source and the gamma-ray flash likely share a common spatial source distribution. In other words, the gamma-rays came from the same locations that the lightning leaders were at when they emitted the x-rays before the return stroke.

[44] Interestingly, if we use x-ray data from  $-500 \mu\text{s}$  to  $-250 \mu\text{s}$  before the return stroke, instead of data from  $-2000 \mu\text{s}$  to  $-500 \mu\text{s}$ , we find that much more energy is deposited on the detectors on the eastern (right) side of Figure 5, near the inferred lightning strike location. We also find that the agreement between the gamma-ray flash and the lightning x-ray data worsens significantly, indicating that the leader branches that are not directly involved in the attachment process are more likely the source of the gamma-rays.

[45] Previous time-of-arrival (TOA) observations that compare fast electric field pulses from the leader step formation with the x-ray emission, show that the x-rays are

spatially and temporally collocated with the leader steps [*Howard et al.*, 2008]. Combining this fact with our new results, suggests that the leaders, recorded  $-2000$  to  $-500 \mu\text{s}$  before the return stroke are also the source of the gamma-ray flash. However, the gamma-ray flash occurred  $191 \mu\text{s}$  after the start of the return stroke while the current near the ground was still large (see Figure 7). With a typical propagation speed of  $1-2 \times 10^8 \text{ m/s}$  [*Rakov and Uman*, 2003], the return stroke current wave had sufficient time to propagate to all other branches of the lightning. As a result, negative leader propagation, which generated the x-rays before the return stroke, is not expected to be occurring at the time of the gamma-ray flash.

## 4.2. Energy Spectrum

[46] We end this section with a discussion of the energy spectrum. Because of the limited statistic (17 photons), it is not possible to make a detailed energy spectrum of the gamma-ray flash. Nevertheless, six coarse energy bins may be plotted, which contain enough information to perform a statistical analysis to test the underlying source mechanisms (e.g., cold runaway electron production versus RREAs). Figure 6 shows the counts per unit energy for the gamma-ray flash. Also shown are the accumulated counts spectrum for TGFs measured by the RHESSI spacecraft as published in *Dwyer and Smith* [2005] and the x-rays from the lightning leader that preceded the flash between  $-2000 \mu\text{s}$  and  $-500 \mu\text{s}$ . As discussed above, x-ray pulses from the lightning leaders show signs of pulse pile up, so the energy spectrum for the lightning likely over estimates the number of high energy photons and underestimates the number of low energy photons. This spectrum is shown in Figure 6. The upper dash-dotted curve at the bottom of the plot is the model x-ray spectrum at the source inferred by the work by *Saleh et al.* [2009] for a bright rocket triggered lightning dart stepped leader. The spectrum inferred by *Dwyer et al.* [2004b] (lower dash-dotted curve) is even softer, showing some of the variability of the x-ray spectrum from lightning. The observed spectrum appears to fall in between these two previous estimates.

[47] As can be seen, the gamma-ray flash matches the TGF data much more closely than the lightning data and is composed of much higher energy photons than ever reported in association from lightning. The RHESSI TGF data has been found to be well fit with the RREA spectrum, and since the RREA spectrum has a characteristic energy of about 7 MeV, insensitive to most properties of the source region, including of the electric field strengths and air densities, this suggests that the gamma-ray flash was also produced by the RREA mechanism and not just cold runaway as is thought to occur during lightning [*Dwyer*, 2004].

[48] Monte Carlo simulations were used to calculate the gamma-ray spectrum on the ground for both a downward RREA beam and a downward positron beam for several source altitudes. If the lightning leaders are really the source of the gamma-ray flash, then they were probably not more than several hundred meters above the ground, since above that height the spatial variation seen in the data would be washed out and the flux of x-rays would have been very low. We consider a source 400 m above the ground with a uniform vertical field (either pointed up or down) in the source region with a magnitude of 700 kV/m. The choice of the

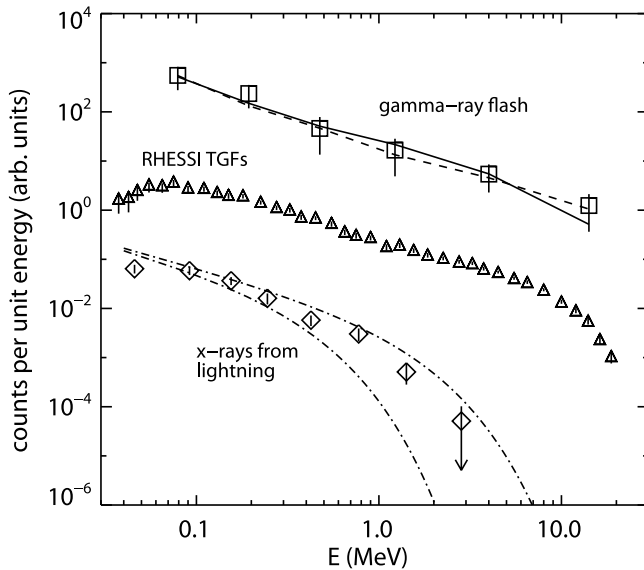


**Figure 6.** Energy spectrum of the gamma-ray flash (squares), along with the RREA model fit (solid curve) and the runaway positron model fit (dashed curve). The number of counts that are in each data point of the gamma-ray flash are, from left to right, 4, 4, 2, 2, 3 and 2. The triangles show the accumulated TGF counts spectrum measured by the RHESSI spacecraft [from *Dwyer and Smith, 2005*]. The diamonds show the energy spectrum of pulses measured for the natural lightning leader for times between  $-2000$  and  $-500$   $\mu\text{s}$  before the return stroke. Due to pulse pile-up the true x-ray spectrum from the lightning will likely be softer than that plotted. The dashed dotted curves at the bottom of the figure show the estimated energy spectra (at the source) found by *Dwyer et al. [2004b]* (bottom curve) and *Saleh et al. [2009]* (top curve). As can be seen, the gamma-ray flash agrees with the RREA and positron spectra and resembles the TGF data but not the spectra of x-rays from lightning.

electric field is somewhat arbitrary, since the energy spectra of the runaway electrons and resulting bremsstrahlung photons depend only weakly upon the field magnitude [*Dwyer and Smith, 2005*]. For a downward directed RREA, energetic seed electrons with an energy of 100 keV are injected at the top of the avalanche region and allowed to propagate downward through 6 avalanche lengths, experiencing avalanche multiplication. For a 700 kV/m field, the avalanche length is about 16.5 m, so in the simulation the total avalanche region had a length of about 100 m. Higher fields produce smaller avalanche length and hence shorter avalanche regions. The seed particles could, in principle, come from atmospheric cosmic ray particles, cold runaway electron production in the high fields associated with leaders and/or streamers, or from the relativistic feedback mechanism. Below, we shall show that only the latter two mechanisms, cold runaway and relativistic feedback, are viable. All the particles in the simulation are allowed to exit the source region and propagated until their energy falls below 30 keV. Positrons, which might be the result of relativistic feedback, are simulated in a similar manner, with the particles injected at the top of a downward pointing high field region (opposite the previous case) and allowed to

propagate downward until they exit the high field region and stop. Unlike the runaway electrons, the runaway positrons do not avalanche multiply. However, their average energy is much larger than the 7 MeV average energy of the runaway electrons [*Dwyer, 2012*]. As a result, the bremsstrahlung spectrum generated by the positrons extends to higher energies than from the runaway electrons. We note that for a source height less than a few hundred meters, some of the energetic positrons may reach the ground, so it is possible that some of the largest pulses detected during the gamma-ray flash were produced by energetic charged particles and not by gamma-rays.

[49] The bremsstrahlung x-rays and gamma-rays generated by the runaway electrons and positrons are propagated through the air until they reach the ground. Absorption and backscatter of the gamma-rays in the soil are included. All photons are recorded within a 350 m radius of the foot point of the beam, corresponding to the same area as covered by TERA at the ICLRT. For more details on the Monte Carlo simulations see *Dwyer and Smith [2005]*. The fits of the Monte Carlo simulations are shown in Figure 6. The solid curve is for a downward directed RREA and the dashed curve is for downward directed positrons (upward RREAs). As can be seen, both positron and electron models fit the data well. It was also found that other altitudes up to 2 km give reasonably good fits. It can be concluded that the source mechanism likely does involve RREAs, either directed upward or downward, since the high energies imply that runaway electron avalanche multiplication is occurring. In fact, the detection of a  $>20$  MeV gamma-ray shows that there was a minimum of 3 avalanche lengths present in the source region, since runaway electrons gain about 7 MeV per avalanche length [see *Dwyer, 2008*]. Indeed, there were probably more than 3 avalanche lengths, since 1 in 17 recorded photons were over 20 MeV, suggesting that a substantial number of energetic electrons or positrons had energies over 20 MeV. For example, for 4 avalanche lengths, the fraction of  $>20$  MeV gamma-rays recorded at the ground is only 0.0014, compared with the measure ratio of 0.12. When 6 avalanche lengths are simulated, the fraction of  $>20$  MeV gamma-rays recorded at the ground is 0.006. This suggests that if a downward beam of runaway electrons is generating the gamma-rays then a significant amount of RREA multiplication was occurring in the source region, with many avalanche lengths likely. However, even with 6 or more avalanche lengths the probability of measuring a photon in excess of 20 MeV in this case is less than 10% for a downward directed RREA. Therefore, the measurement of the 20 MeV particle (either a gamma-ray or a positron) is more naturally explained by the downward positron model, since the positrons have a much higher average energy than the runaway electrons [*Dwyer, 2012*]. Furthermore, 6 avalanche lengths is within the range of avalanche lengths for which relativistic feedback may become self-sustaining, i.e., over the feedback threshold, adding support that relativistic feedback is a reasonable mechanism for explaining the gamma-ray flash.

[50] Monte Carlo simulations for a source 400 m above the ground gives the estimate that there were approximately  $8 \times 10^9$  runaway electrons at the source if the RREA were beamed down and  $3 \times 10^7$  runaway positrons if the RREA was beamed up. Considering that there are typically several

thousand runaway electrons for every runaway positron generated, an upward RREA may have contained over  $10^{11}$  runaway electrons. If the source altitude were in fact higher then these numbers would be larger. These numbers of runaway electrons are lower than the  $\sim 10^{17}$  for TGFs seen from space, but it is not known how they compare to the real average of TGF population, due to the detection thresholds of the space instruments [Østgaard et al., 2012].

## 5. Discussion

[51] In this paper, we have shown that the gamma-ray flash observed on June 30, 2009 at the ICLRT had an energy spectrum and duration consistent with TGFs seen from space. This energy spectrum shows that RREA was almost certainly involved in the production of these gamma-rays, similar to TGFs. Because this ground level event satisfies the standard definition of a TGF: a short, intense burst of multi-MeV gamma-rays produced in association with thundercloud and lightning, we suggest that this event is indeed a ground-level terrestrial gamma-ray flash, the second ever recorded.

[52] While other observations have found gamma-ray glows from thunderclouds with energy spectra consistent with RREA, these glows, which last seconds to many minutes, have much longer durations and usually have lower fluxes than the event presented here [Alexeenko et al., 2002; Brunetti et al., 2000; Chilingarian et al., 2010; Chubenko et al., 2000; Torii et al., 2002, 2009, 2011; Tsuchiya et al., 2007, 2009, 2011].

[53] It is instructive to compare the number of runaway electrons and positrons to the number of seed particles available to initiate RREAs. The flux of atmospheric cosmic ray particles at 400 m above the ground that may serve as seeds is about  $200 \text{ m}^{-2} \text{ s}^{-1}$  [Hillas, 1972]. The part of the ICLRT covered by TERA has a total area of about  $4 \times 10^5 \text{ m}^2$ . Therefore, in  $53 \mu\text{s}$  we expect about 4000 seed particles for this area. Because of the spatial structure seen in the gamma-ray flash, it is unlikely that the source region is uniform over this area. More likely, the area of the source region(s) is much smaller, so this number of seed is probably an upper limit. Using the Monte Carlo result that there was either  $8 \times 10^9$  downward runaway electrons at the source or  $3 \times 10^7$  downward runaway positrons. This implies that the ratio of runaway electrons to cosmic ray seeds is  $>2 \times 10^6$ , and the ratio of positrons to seeds is  $>7500$ . The former implies that the avalanche multiplication factor is  $>2 \times 10^6$ , which is over the relativistic feedback threshold [Dwyer, 2003, 2007, 2008]. The latter implies that the RREAs generated by the positrons exceed the RREAs generated by cosmic rays by a factor of 7500, again suggesting that relativistic feedback is the dominate mechanism for generating energetic particles. In summary, cosmic rays may be ruled out as the sole source of seed particles. The  $53 \mu\text{s}$  duration also shows that cosmic ray extensive air showers are not playing an important role in generating the gamma-ray flash. This leaves either the relativistic feedback mechanism or the cold runaway electron mechanism seeding RREAs [Gurevich, 1961; Dwyer, 2008; Carlson et al., 2010; Celestin and Pasko, 2011, 2012]. Furthermore, the number of avalanche lengths inferred from the spectrum (see above) suggests that large amounts of avalanche multiplication are occurring, so the source is solidly in the regime in which RREA is important. Both the cold runaway mechanism and the relativistic

feedback mechanism have also been hypothesized to produce TGFs [Dwyer, 2008]. Moreover, Dwyer [2008] argued that these are the only two viable mechanisms for explaining TGFs. Therefore, the observations suggest that the gamma-ray flash may share the same production mechanism as TGFs.

[54] Inspection of the optical and field data at the time of the ground level flash did not show anything unusual. Figure 7 shows the magnetic field data for two directions recorded during the flash (station B-24). The current pulses associated with the leader steps are easily seen on the left side of the figure, before the start of the return stroke at approximately  $t = 0$ . The vertical dashed lines show the time period that the gamma-ray flash occurred. As can be seen the magnetic field deflection was still large at the time of the gamma-ray flash, indicating that substantial current was still flowing along the channel. A small negative deflection can be seen in the east-west magnetic field waveform (red) at the time of the gamma-ray flash. However, it is not clear whether this feature is significant, since it is comparable to other fluctuations in the waveform. Also, no leader activity is evident during the gamma-ray flash. Therefore, the gamma-ray flash appears to occur at the later stage of a decaying return stroke with no evidence of local leader activity at that time. Although some distant sferics observations of lightning associated with TGFs found large sferics similar in size to CG strokes [Cohen et al., 2010], there has not been any previous direct evidence of an association of a TGF with a CG lightning stroke. Indeed, most recent modeling of TGFs has assumed that the TGF occurs during the leader propagation inside the thundercloud and not during a return stroke [Dwyer, 2012; Carlson et al., 2010; Celestin and Pasko, 2011, 2012].

[55] We conclude with a suggestion for how the ground level gamma-ray flash may have occurred. Based upon the analysis presented in this paper, we conclude that the gamma-ray flash probably came from the network of defunct lightning leaders over the ICLRT, which had produced the x-ray emission while propagating downward before the return stroke, but had since stopped propagating after the start of the stroke. If the electric fields in the streamer zones around the defunct lightning leaders had discharged at about the time of the return stroke, then most of the negative charge carried by the leaders would reside at the outer boundary of the streamer zones, well away from the locations of the leader channels and tips. During the return stroke, the lightning channels quickly reach ground potential, thus placing positive charge on the defunct leader tips and causing the electric fields in the streamer zones to reverse and reach large magnitudes. We note that even if the electric field around the defunct leader channels is directed downward, due to the positive charge that is added to the old leader tips, the electric field measured on the ground could still be directed upward, since there could still be a net negative charge overhead. These electric fields near the leader tips may cause RREA multiplication, augmented by either cold runaway electron emission or relativistic feedback, possibly generating the observed gamma-ray flash. As an example, if 6 avalanche lengths were present in the high field region then the electric potential difference in this region must be at least 40 MV, since about 7 MV are required per avalanche length in strong fields. For a 50 m streamer zone, this then gives an average field of 800 kV/m in the avalanche region. In this scenario the electric fields would be approximately radial, centered on

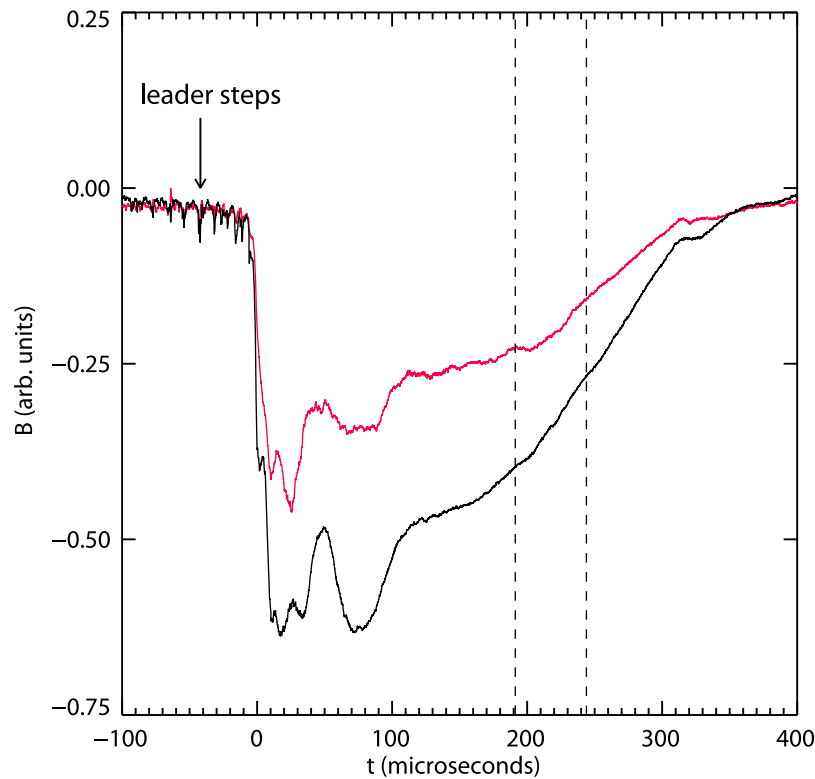


**Figure 7.** Magnetic field measurements made at station 24 at the ICLRT (see Figures 4 and 5). The red curve is horizontal magnetic fields in the east-west direction and the black curve is the horizontal magnetic field in the north-south direction. The negative deflection starting at about  $t = 0$  is due to the return stroke current. The small negative pulses on the left side of the plot are due to the leader steps. The time of the gamma-ray flash is between the vertical dashed lines.

each defunct leader tip. This geometry is very favorable for relativistic feedback, since the avalanches on one side of the leader tip can generate secondary avalanches on the other side without the x-rays and positrons having to turn around in the electric field. This type of feedback was named “cross-fire” feedback by Dwyer [2007]. Further work is still required to quantify the relativistic feedback rates for this geometry [Kutsyk et al., 2011], and detailed modeling is needed to see if large enough electric fields may be generated near the defunct leader tips during the return stroke.

[56] **Acknowledgments.** We wish to thank U. Abdulla for useful discussions. This work was supported in part by DARPA grants HR0011-08-1-0088 and HR0011-1-10-1-0061.

[57] Robert Lysak thanks the reviewers for their assistance in evaluating this paper.

## References

- Alexeenko, V. V., N. S. Khaerdinov, A. S. Lidvansky, and V. B. Petkov (2002), Transient variations of secondary cosmic rays due to atmospheric electric field and evidence for pre-lightning particle acceleration, *Phys. Lett. A*, *301*, 299–306, doi:10.1016/S0375-9601(02)00981-7.
- Boyle, P., R. Flowerdew, and A. Williams (1997), Evaluating the goodness of fit in models of sparse medical data: A simulation approach, *Int. J. Epidemiol.*, *26*(3), 651–656, doi:10.1093/ije/26.3.651.
- Briggs, M. S., et al. (2010), First results on terrestrial gamma ray flashes from the Fermi Gamma-ray Burst Monitor, *J. Geophys. Res.*, *115*, A07323, doi:10.1029/2009JA015242.
- Briggs, M. S., et al. (2011), Electron-positron beams from terrestrial lightning observed with Fermi GBM, *Geophys. Res. Lett.*, *38*, L02808, doi:10.1029/2010GL046259.
- Brunetti, M., S. Cecchini, M. Galli, G. Giovannini, and A. Pagliarini (2000), Gamma-ray bursts of atmospheric origin in the MeV energy range, *Geophys. Res. Lett.*, *27*, 1599–1602, doi:10.1029/2000GL003750.
- Carlson, B. E., N. G. Lehtinen, and U. S. Inan (2007), Constraints on terrestrial gamma ray flash production from satellite observation, *Geophys. Res. Lett.*, *34*, L08809, doi:10.1029/2006GL029229.
- Carlson, B., N. Lehtinen, and U. Inan (2010), Terrestrial gamma ray flash production by active lightning leader channels, *J. Geophys. Res.*, *115*, A10324, doi:10.1029/2010JA015647.
- Celestin, S., and V. P. Pasko (2011), Energy and fluxes of thermal runaway electrons produced by exponential growth of streamers during the stepping of lightning leaders and in transient luminous events, *J. Geophys. Res.*, *116*, A03315, doi:10.1029/2010JA016260.
- Celestin, S., and V. P. Pasko (2012), Compton scattering effects on the duration of terrestrial gamma-ray flashes, *Geophys. Res. Lett.*, *39*, L02802, doi:10.1029/2011GL050342.
- Chilingarian, A., A. Daryan, K. Arakelyan, A. Hovhannisyanyan, B. Mailyan, L. Melkumyan, G. Hovsepyan, S. Chilingaryan, A. Reymers, and L. Vanyan (2010), Ground-based observations of thunderstorm-correlated fluxes of high-energy electrons, gamma rays, and neutrons, *Phys. Rev. D*, *82*(4), 043009.
- Chubenko, A. P., V. P. Antonova, S. Y. Kryukov, V. V. Piskal, M. O. Ptitsyn, A. L. Shepetov, L. I. Vildanova, K. P. Zybin, and A. V. Gurevich (2000), Intense x-ray emission bursts during thunderstorms, *Phys. Lett. A*, *275*, 90–100, doi:10.1016/S0375-9601(00)00502-8.
- Cohen, M. B., U. S. Inan, R. K. Said, and T. Gjestland (2010), Geolocation of terrestrial gamma-ray flash source lightning, *Geophys. Res. Lett.*, *37*, L02801, doi:10.1029/2009GL041753.
- Cummer, S. A., Y. Zhai, W. Hu, D. M. Smith, L. I. Lopez, and M. A. Stanley (2005), Measurements and implications of the relationship between lightning and terrestrial gamma ray flashes, *Geophys. Res. Lett.*, *32*, L08811, doi:10.1029/2005GL022778.
- Cummer, S. A., G. Lu, M. S. Briggs, V. Connaughton, S. Xiong, G. J. Fishman, and J. R. Dwyer (2011), The lightning-TGF relationship on microsecond timescales, *Geophys. Res. Lett.*, *38*, L14810, doi:10.1029/2011GL048099.

- Dwyer, J. R. (2003), A fundamental limit on electric fields in air, *Geophys. Res. Lett.*, *30*(20), 2055, doi:10.1029/2003GL017781.
- Dwyer, J. R. (2004), Implications of x-ray emission from lightning, *Geophys. Res. Lett.*, *31*, L12102, doi:10.1029/2004GL019795.
- Dwyer, J. R. (2005), The initiation of lightning by runaway air breakdown, *Geophys. Res. Lett.*, *32*, L20808, doi:10.1029/2005GL023975.
- Dwyer, J. R. (2007), Relativistic breakdown in planetary atmospheres, *Phys. Plasmas*, *14*(4), 042901, doi:10.1063/1.2709652.
- Dwyer, J. R. (2008), Source mechanisms of terrestrial gamma-ray flashes, *J. Geophys. Res.*, *113*, D10103, doi:10.1029/2007JD009248.
- Dwyer, J. R. (2012), The relativistic feedback discharge model of terrestrial gamma ray flashes, *J. Geophys. Res.*, *117*, A02308, doi:10.1029/2011JA017160.
- Dwyer, J. R., and D. M. Smith (2005), A comparison between Monte Carlo simulations of runaway breakdown and terrestrial gamma-ray flash observations, *Geophys. Res. Lett.*, *32*, L22804, doi:10.1029/2005GL023848.
- Dwyer, J. R., et al. (2003), Energetic radiation produced during rocket-triggered lightning, *Science*, *299*, 694–697, doi:10.1126/science.1078940.
- Dwyer, J. R., et al. (2004a), A ground level gamma-ray burst observed in association with rocket-triggered lightning, *Geophys. Res. Lett.*, *31*, L05119, doi:10.1029/2003GL018771.
- Dwyer, J. R., et al. (2004b), Measurements of x-ray emission from rocket-triggered lightning, *Geophys. Res. Lett.*, *31*, L05118, doi:10.1029/2003GL018770.
- Dwyer, J. R., et al. (2005), X-ray bursts associated with leader steps in cloud-to-ground lightning, *Geophys. Res. Lett.*, *32*, L01803, doi:10.1029/2004GL021782.
- Dwyer, J. R., B. W. Grefenstette, and D. M. Smith (2008a), High-energy electron beams launched into space by thunderstorms, *Geophys. Res. Lett.*, *35*, L02815, doi:10.1029/2007GL032430.
- Dwyer, J. R., Z. Saleh, H. K. Rassoul, D. Concha, M. Rahman and V. Cooray, J. Jerauld, M. A. Uman, and V. A. Rakov (2008b), A study of X-ray emission from laboratory sparks in air at atmospheric pressure, *J. Geophys. Res.*, *113*, D23207, doi:10.1029/2008JD010315.
- Dwyer, J. R., D. M. Smith, M. A. Uman, Z. Saleh, B. Grefenstette, B. Hazelton, and H. K. Rassoul (2010), Estimation of the fluence of high-energy electron bursts produced by thunderclouds and the resulting radiation doses received in aircraft, *J. Geophys. Res.*, *115*, D09206, doi:10.1029/2009JD012039.
- Dwyer, J. R., M. Schaal, H. K. Rassoul, M. A. Uman, D. M. Jordan, D. Hill, and H. K. Rassoul (2011), High-speed X-ray images of triggered lightning dart leaders, *J. Geophys. Res.*, *116*, D20208, doi:10.1029/2011JD015973.
- Evans, M. J., and J. S. Rosenthal (2004), *Probability and Statistics: The Science of Uncertainty*, W. H. Freeman, New York.
- Fishman, G. J., et al. (1994), Discovery of intense gamma-ray flashes of atmospheric origin, *Science*, *264*, 1313–1316, doi:10.1126/science.264.5163.1313.
- Fishman, G. J., et al. (2011), Temporal properties of the terrestrial gamma-ray flashes from the Gamma-Ray Burst Monitor on the Fermi Observatory, *J. Geophys. Res.*, *116*, A07304, doi:10.1029/2010JA016084.
- Gjosteland, T., N. Østgaard, P. H. Connell, J. Stadsnes, and G. J. Fishman (2010), Effects of dead time losses on terrestrial gamma ray flash measurements with the Burst and Transient Source Experiment, *J. Geophys. Res.*, *115*, A00E21, doi:10.1029/2009JA014578.
- Grefenstette, B. W., D. M. Smith, J. R. Dwyer and G. J. Fishman (2008), Time evolution of terrestrial gamma ray flashes, *Geophys. Res. Lett.*, *35*, L06802, doi:10.1029/2007GL032922.
- Gurevich, A. V. (1961), On the theory of runaway electrons, *Sov. Phys. JETP, Engl. Transl.*, *12*(5), 904–912.
- Gurevich, A. V., and K. P. Zybin (2001), Runaway breakdown and electric discharges in thunderstorms, *Phys. Uspekhi*, *44*, 1119, doi:10.1070/PU2001v044n11ABEH000939.
- Gurevich, A. V., G. M. Milikh, and R. A. Roussel-Dupré (1992), Runaway electron mechanism of air breakdown and preconditioning during a thunderstorm, *Phys. Lett. A*, *165*, 463–468, doi:10.1016/0375-9601(92)90348-P.
- Hauschild, T., and M. Jentschel (2001), Comparison of maximum likelihood estimation and chi-square statistics applied to counting experiments, *Nucl. Instrum. Methods Phys. Res., Sect. A*, *457*, 384–401, doi:10.1016/S0168-9002(00)00756-7.
- Hazelton, B. J., B. W. Grefenstette, D. M. Smith, J. R. Dwyer, X.-M. Shao, S. A. Cummer, T. Chronis, E. H. Lay, and R. H. Holzworth (2009), Spectral dependence of terrestrial gamma-ray flashes on source distance, *Geophys. Res. Lett.*, *36*, L01108, doi:10.1029/2008GL035906.
- Hill, J. D., M. A. Uman, D. M. Jordan, J. R. Dwyer, and H. Rassoul (2012), “Chaotic” dart leaders in triggered lightning: Electric fields, X-rays, and source locations, *J. Geophys. Res.*, *117*, D03118, doi:10.1029/2011JD016737.
- Hillas, A. M. (1972), *Cosmic Rays*, Pergamon, Oxford, U. K.
- Howard, J., M. A. Uman, J. R. Dwyer, D. Hill, C. Biagi, Z. Saleh, J. Jerauld, H. K. Rassoul (2008), Co-location of lightning leader x-ray and electric field change sources, *Geophys. Res. Lett.*, *35*, L13817, doi:10.1029/2008GL034134.
- Humphrey, P. J., W. Liu, and D. A. Buote (2009),  $\chi^2$  and Poissonian data: Biases even in the high-count regime and how to avoid them, *Astrophys. J.*, *693*, 822–829, doi:10.1088/0004-637X/693/1/822.
- Inan, S. U., S. C. Reising, G. J. Fishman, and J. M. Horack (1996), On the association of terrestrial gamma-ray bursts with lightning and implications for sprites, *Geophys. Res. Lett.*, *23*, 1017–1020, doi:10.1029/96GL00746.
- Jerauld, J. (2007), Properties of natural cloud-to-ground lightning inferred from multiple-station measurements of close electric and magnetic fields and field derivatives, PhD dissertation, Univ. of Fla., Gainesville.
- Kutsyk, I. M., L. P. Babich, and E. N. Donskoi (2011), Self-sustained relativistic-runaway-electron avalanches in the transverse field of lightning leader as sources of terrestrial gamma-ray flashes, *JETP Lett.*, *94*(8), 606–609, doi:10.1134/S0021364011200094.
- Lehtinen, N. G., T. F. Bell, and U. S. Inan (1999), Monte Carlo simulation of runaway MeV electron breakdown with application to red sprites and terrestrial gamma ray flashes, *J. Geophys. Res.*, *104*, 24,699–24,712, doi:10.1029/1999JA900335.
- Lu, G., R. J. Blakeslee, J. Li, D. M. Smith, X.-M. Shao, E. W. McCaul, D. E. Buechler, H. J. Christian, J. M. Hall, and S. A. Cummer (2010), Lightning mapping observation of a terrestrial gamma-ray flash, *Geophys. Res. Lett.*, *37*, L11806, doi:10.1029/2010GL043494.
- Mighell, K. J. (1999), Parameter estimation in astronomy with Poisson-distributed data. I. The  $\chi^2$  statistic, *Astrophys. J.*, *518*, 380–393, doi:10.1086/307253.
- Moss, G. D., V. P. Pasko, N. Liu, and G. Veronis (2006), Monte Carlo model for analysis of thermal runaway electrons in streamer tips in transient luminous events and streamer zones of lightning leaders, *J. Geophys. Res.*, *111*, A02307, doi:10.1029/2005JA011350.
- Østgaard, N., T. Gjosteland, B. E. Carlson, R. S. Hansen, and A. B. Collier (2012), The true fluence distribution of terrestrial gamma flashes at satellite altitude, *J. Geophys. Res.*, *117*, A03327, doi:10.1029/2011JA017365.
- Rakov, V. A., and M. A. Uman (2003), *Lightning: Physics and Effects*, Cambridge Univ. Press, Cambridge, U. K.
- Saleh, Z., J. Dwyer, J. Howard, M. Uman, M. Bakhtiari, D. Concha, M. Stapleton, D. Hill, C. Biagi, and H. Rassoul (2009), Properties of the X-ray emission from rocket-triggered lightning as measured by the Thunderstorm Energetic Radiation Array (TERA), *J. Geophys. Res.*, *114*, D17210, doi:10.1029/2008JD011618.
- Shao, X.-M., T. Hamlin, and D. M. Smith (2010), A closer examination of terrestrial gamma-ray flash-related lightning processes, *J. Geophys. Res.*, *115*, A00E30, doi:10.1029/2009JA014835.
- Smith, D. M., et al. (2011), A terrestrial gamma ray flash observed from an aircraft, *J. Geophys. Res.*, *116*, D20124, doi:10.1029/2011JD016252.
- Stanley, M., et al. (2006), A link between terrestrial gamma-ray flashes and intracloud lightning discharges, *Geophys. Res. Lett.*, *33*, L06803, doi:10.1029/2005GL025537.
- Torii, T., M. Takeishi, and T. Hosono (2002), Observation of gamma-ray dose increase associated with winter thunderstorm and lightning activity, *J. Geophys. Res.*, *107*(D17), 4324, doi:10.1029/2001JD000938.
- Torii, T., T. Sugita, S. Tanabe, Y. Kimura, M. Kamogawa, K. Yajima, and H. Yasuda (2009), Gradual increase of energetic radiation associated with thunderstorm activity at the top of Mt. Fuji, *Geophys. Res. Lett.*, *36*, L13804, doi:10.1029/2008GL037105.
- Torii, T., T. Sugita, M. Kamogawa, Y. Watanabe, and K. Kusunoki (2011), Migrating source of energetic radiation generated by thunderstorm activity, *Geophys. Res. Lett.*, *38*, L24801, doi:10.1029/2011GL049731.
- Tsuchiya, H., et al. (2007), Detection of high-energy gamma rays from winter thunderclouds, *Phys. Rev. Lett.*, *99*, 165002, doi:10.1103/PhysRevLett.99.165002.
- Tsuchiya, H., et al. (2009), Observation of an energetic radiation burst from mountain-top thunderclouds, *Phys. Rev. Lett.*, *102*, 255003, doi:10.1103/PhysRevLett.102.255003.
- Tsuchiya, H., et al. (2011), Long-duration  $\gamma$  ray emissions from 2007 and 2008 winter thunderstorms, *J. Geophys. Res.*, *116*, D09113, doi:10.1029/2010JD015161.
- Williams, E., et al. (2006), Lightning flashes conducive to the production and escape of gamma radiation to space, *J. Geophys. Res.*, *111*, D16209, doi:10.1029/2005JD006447.